

Abstract

The hydraulic fracture of ice during the rapid tapping of supraglacial lakes is proposed as one mechanism to establish efficient surface-to-bed hydraulic pathways through kilometre-thick ice. This study presents detailed records of lake discharge, ice motion, and passive seismicity capturing the behaviour and processes preceding, during and following the rapid (~ 2 h) tapping of a large ($\sim 4 \text{ km}^2$) supraglacial lake through 1.1 km of the western margin of the Greenland Ice Sheet. Peak discharge ($3300 \text{ m}^3 \text{ s}^{-1}$) was coincident with maximal rates of horizontal displacement and vertical uplift, indicating that surface water accessed the ice-bed interface causing widespread hydraulic separation and enhanced basal motion. The differential motion of four GPS located around the lake, record the opening and closure of fractures suggesting that on short time-scales the brittle fracture of ice dominates ice flow. We hypothesise that during lake tapping, drainage occurred through a ~ 3 km long longitudinal fracture with a mean width of ~ 0.4 m. The perennial location of the supraglacial lake and the observed pattern of fracturing and surface uplift evince control by the local subglacial topography and the gradient of hydraulic potential. Our observations support the assertion that water-filled crevasses can propagate without longitudinal extension. The tapping of the lake coincided with the rapid drainage of a cluster of supraglacial lakes located within the same elevation band coincident with a notable and isolated peak in the catchment-wide, proglacial Watson River hydrograph.

1 Introduction

Variations in the delivery of surface water to the base of the Greenland Ice Sheet induces fluctuations in ice sheet velocity on inter-annual, seasonal, diurnal and sub-diurnal lake tapping time scales (Zwally et al., 2002; van de Wal et al., 2008; Bartholomew et al., 2011; Shepherd et al., 2009; Das et al., 2008; Hoffman et al., 2011). For water to access the bed of the Greenland Ice Sheet a hydraulic pathway must first

TCD

6, 3863–3889, 2012

Rapid lake tapping, W. Greenland

S. H. Doyle et al.

Title Page

Abstract

Introduction

Conclusions

References

Tables

Figures

◀

▶

◀

▶

Back

Close

Full Screen / Esc

Printer-friendly Version

Interactive Discussion



be established through often kilometre-thick ice. Given sufficient water supply, a water-filled fracture will propagate to the base of an ice mass when the overburden stress at the fracture tip is offset by the density contrast between ice and water (Weertman, 1973; Alley et al., 2005; van der Veen, 2007).

5 Krawczynski et al. (2009) calculated that supraglacial lakes 250 to 800 m across and 2 to 5 m deep contain sufficient water to drive a fracture to the base of kilometre-thick ice. Many lakes on the Greenland Ice Sheet attain this size or larger (Box and Ski, 2007; Echelmeyer et al., 1991; Georgiou et al., 2009) of which a small proportion (13% between 2005–2009) drain in less than 2 days (Selmes et al., 2011). Surface
10 lakes can drain rapidly via supraglacial rivers and moulins, however many drain by the in situ propagation of hydraulically driven fractures (e.g. Das et al., 2008), here termed lake tapping.

Lake tapping events provide water fluxes that exceed the capacity of the subglacial drainage system, leading to transient high subglacial water pressures, hydraulic jacking and ice sheet acceleration (Bartholomaeus et al., 2008; Das et al., 2008; Pimental and Flowers, 2010). The integrated effect of multiple lake tapping events, and continued water flow into the hydraulic pathways they create, have the capacity to increase the Greenland Ice Sheet's negative mass-balance and sea level contribution, by accelerating ice to lower, and therefore warmer, elevations – a process termed dynamic thinning
20 (Bamber et al., 2007; Pritchard et al., 2009).

Whilst lake tapping events represent major perturbations of the subglacial hydrological system and provide natural experiments for process-based investigations of glacier-hydromechanics, few studies have succeeded in capturing them. Boon and Sharp (2003) measured premonitory drainage events preceding the complete drainage
25 of a 6.9 m deep supraglacial pond through a 150 m thick Arctic glacier on Ellesmere Island. Das et al. (2008) observed horizontal and vertical ice motion and seismicity during the rapid (~ 1.4 h) tapping of a large supraglacial lake via hydrofracture through 980 m of ice to the bed of the Greenland Ice Sheet. This study presents detailed ice motion,

**Rapid lake tapping,
W. Greenland**

S. H. Doyle et al.

Title Page

Abstract

Introduction

Conclusions

References

Tables

Figures

◀

▶

◀

▶

Back

Close

Full Screen / Esc

Printer-friendly Version

Interactive Discussion



lake volume change, and seismic time series capturing the rapid tapping of a large
5 supraglacial lake through 1.1 km of the western margin of the Greenland Ice Sheet.

2 Field site and methods

The field site, Lake F (67.01° N 48.74° W), is located 70 km from the terminus of Rus-
sell Glacier, West Greenland (Fig. 1). Russell Glacier catchment represents a typical
land-terminating sector of the Greenland Ice Sheet which, during the melt-season ac-
cumulates supraglacial lakes (McMillan et al., 2007) and shows diurnal and seasonal
10 covariations in ice velocity and surface uplift (Bartholomew et al., 2011). Lake F is sit-
uated at the head of a fast flow unit where summer ice surface velocities attain 300 %
above the winter mean (see Fig. 3 of Palmer et al., 2011).

Remote sensing observations indicate annually repeated growth and rapid drainage
15 of Lake F in the same location, with a mean date of drainage between 2002 and 2009
of 14 July. During the abnormally warm melt seasons of 2003, 2007 and 2010 (see
Cappelen et al., 2001; Cappelen, 2011) Lake F tapped 3 to 4 weeks earlier compared
to other years in the 2002 to 2010 period.

On 26 June 2010, Lake F was instrumented with four GPS, six seismometers and
20 two water level sensors. Five days later at 01:40 on the 30 June, the lake drained com-
pletely in ~ 2 h. Following drainage, the bathymetry of the lake bed and the locations
of fractures and moulins were surveyed. Lake volume (V) and discharge (Q) are esti-
mated by combining water level measurements with the lake bathymetry. All times are
expressed in Coordinated Universal Time (UTC) which is two hours ahead of local time
25 in summer.

2.1 Measurements of ice motion

Four dual-frequency GPS receivers (Trimble R7 and Leica SR520) were installed sur-
rounding Lake F (Fig. 2). GPS antennae were installed on 6 m poles drilled 5 m into the

Rapid lake tapping, W. Greenland

S. H. Doyle et al.

Title Page

Abstract

Introduction

Conclusions

References

Tables

Figures

◀

▶

◀

▶

Back

Close

Full Screen / Esc

Printer-friendly Version

Interactive Discussion



**Rapid lake tapping,
W. Greenland**

S. H. Doyle et al.

Title Page

Abstract

Introduction

Conclusions

References

Tables

Figures

I◀

▶I

◀

▶

Back

Close

Full Screen / Esc

Printer-friendly Version

Interactive Discussion



ice, which subsequently freeze in and thereafter provide a record of 3-dimensional ice surface motion. Data, sampled continuously at a 10 s interval, were processed against a bedrock-mounted reference station using the differential phase kinematic positioning software, Track v. 1.24 (Chen, 1998; Herring et al., 2010), and final precise ephemeris from the International GNSS Service (Dow et al., 2009). The reference station was located 1 km from the terminus of Russell Glacier giving baseline lengths ≤ 70 km. To improve solutions at the day boundary, 36 h files were processed and the first and last six hours of the output position time series were discarded. Uncertainties in the positions are estimated at < 0.02 m in the horizontal and < 0.05 m in the vertical. The output position data are characterised by high frequency noise caused by receiver and data processing errors and wind-induced antenna motion. To suppress this high-frequency noise without causing a shift in phase, positions were filtered with a 1 h centred moving average. To quantify differential motion between GPS, relative inter-GPS separation and the rate of separation were calculated from the filtered positions at a 10-min interval.

2.2 Measuring seismic activity

The passive seismic array consisted of six GS-11D geophones with a natural frequency of 4.5 Hz and a bandwidth of 5 to 1000 Hz, continuously recording micro-seismic velocity at a 1 kHz sampling rate on to a RefTek-130 digitiser. To improve coupling with the ice, the geophones were mounted on 15 kg concrete slabs, buried to a depth of 0.3 m and reset every 3 to 5 days before they melted out. For each seismometer, the normalised root mean square (RMS) amplitude was calculated for 1 min time windows using an envelope function after applying a Butterworth filter with a passband of 5 to 50 Hz. To identify step changes in seismicity we calculate the normalised cumulative (seismic) energy from the RMS amplitudes.

2.3 Measurements of lake dynamics

Two pressure transducers (Solinst M15 Levellogger) were installed in Lake F, logging pressure in metres of water head at two minute intervals with a specified accuracy of ± 1 cm (Fig. 2). The records of P1 and P2 were compensated for changes in atmospheric pressure using a third Solinst Levellogger located at GPS1.

Post-tapping, six transects were surveyed across the lake bed with a Leica SR520 GPS recording at 1 Hz. The transects were differentially corrected and interpolated to form a digital elevation model (DEM) of the lake bathymetry with a grid spacing of 10 m. Time series of lake volume (V) and discharge (Q) were calculated by combining the DEM with the water level data. We estimate the uncertainty in the lake volume and discharge at $\pm 8400 \text{ m}^3$ and $\pm 130 \text{ m}^3 \text{ s}^{-1}$, respectively.

To extend the lake volume time series the margin of Lake F was delimited from atmospherically-corrected Moderate-resolution Imaging Spectrometer (MODIS) images allowing lake volume to be calculated from the surveyed bathymetry (Fig. 3). Uncertainty in the MODIS volume calculations, predominantly caused by the difficulty in automatically classifying the lake perimeter from the coarse 250 m resolution imagery, is estimated at $\pm 25\%$.

To investigate the extent and timing of rapid draining lakes within the Russell Glacier catchment, an automatic lake classification was applied to daily-acquired cloud-free MODIS images. Images with partial cloud cover were manually inspected. We define rapid draining as lakes that disappear within a 4 day interval and the date of drainage as the mid-point between the date it was last seen and the date it disappeared. Typically slow-draining lakes took much longer to drain than the 4 day threshold and there is a clear distinction between lakes that drain rapidly (potentially by rapid in situ tapping) and those that drain slowly. Figure 1 shows the date of drainage of rapidly draining lakes and the maximum extent of all lakes across the Russell Glacier catchment in 2010. The drainage network shown in Fig. 1 was created from a 30 m resolution DEM using hydrological modelling software.

TC D

6, 3863–3889, 2012

Rapid lake tapping, W. Greenland

S. H. Doyle et al.

Title Page

Abstract

Introduction

Conclusions

References

Tables

Figures

◀

▶

◀

▶

Back

Close

Full Screen / Esc

Printer-friendly Version

Interactive Discussion



3 Results

3.1 Regional scale lake dynamics

5 Within Russell Glacier catchment in 2010, 45% of the lakes were classified as rapid (< 4 days) draining. The earliest rapid drainage occurred in late-May and the latest in mid-July and in general lower elevation lakes drained earlier than those located at higher elevations. Figure 1 demonstrates that rapid lake drainage events occur in clusters; multiple lakes within the same elevation band drain simultaneously. The rapid tapping of Lake F coincided with the rapid drainage of several adjacent lakes and an isolated peak (30 June to 2 July) in the discharge of catchment-wide proglacial Watson River (see Fig. 8 of van As et al., 2012).

3.2 Formation and drainage of Lake F

15 In 2010, Lake F began to form on 5 June attaining its maximum extent on 24 June with an area of 4.5 km² and a volume of 1.5×10^7 m³ (Fig. 3). Following the installation of the pressure transducers on 26 June the lake volume steadily decreased at a mean rate of 13.8 m³ s⁻¹ from 1.1×10^7 m³ to 7.4×10^6 m³ immediately prior to rapid tapping. This period of low discharge amounts to 3.6×10^6 m³ of water and could be entirely accounted for by two supraglacial rivers discharging into Lake Z and moulin M4 (see Figs. 1 and 2).

20 Rapid tapping (here defined as $Q > 50$ m³ s⁻¹) occurred between 01:40 and 03:15 on the 30 June 2010 with the discharge peaking at $Q_{\max} = 3300$ m³ s⁻¹ at 02:47. Lake F had completely drained by 03:50. Immediately prior to rapid tapping, Lake F had a maximum depth of 9.9 m, an area of 3.8 km² and a volume of 7.4×10^6 m³.

3.3 Observations

25 At 04:50, ~ 0.3 m deep standing water was observed in the centre of the lake overflowing across the clean-cut edge of the main fracture F1. A number of ice blocks had fallen

Title Page

Abstract

Introduction

Conclusions

References

Tables

Figures

◀

▶

◀

▶

Back

Close

Full Screen / Esc

Printer-friendly Version

Interactive Discussion



into F1 or been uplifted by floatation (see Fig. 4a). Fracture F2 was clean cut and open by ~ 0.2 m.

On 1 July, the location, dip and strike of fractures was surveyed. The main fracture, F1, was mapped for 3 km but extended beyond this as a thin (< 1 cm) crack. F1 and F2 were sub-vertical dipping towards the north and west, respectively (Fig. 2). The northern wall of F1 was vertically displaced 0.1 to 0.3 m above the southern wall with the largest vertical offset measured in the deepest region of the lake, 10 m east of M2 (Fig. 4a). Differential vertical displacement was only observed along F1.

Several moulins were also mapped (M1 to 5, Fig. 2). The largest, M1, ~ 10 m in diameter, located on the main fracture F1 near to the intersection with subsidiary fracture F2, was explored to a depth of 45 m below the surface (Fig. 4b). At 45 m, M1 continued vertically downwards but was partially restricted by fallen blocks of ice. Water entering M2 could be heard to flow englacially along the main fracture F1 at a shallow depth before descending vertically down M1.

The main ~ 5 m wide supraglacial river feeding into Lake F from the north was intercepted by a fracture forming three moulins, collectively M3 (Fig. 2). The evolution of M3 was observed over a number of days. Initially, water flowing into the clean-cut fracture began to cut notches. As time progressed the notches became wider and deeper, the fracture closed up, and one moulin captured all the water that was initially draining into three. A similar evolution was observed for M2 which also continued to receive water throughout the melt season. Moulins M1, M4 and M5 were not connected to supraglacial streams after rapid tapping.

3.4 Ice displacement

Figure 5 depicts the complex horizontal and vertical GPS motion preceding, during and following the lake tapping event. The first abnormal GPS motion occurred on 29 June when *south-east* GPS3 accelerated to the west concomitant with ~ 0.2 m of uplift. *North-east* GPS4 and *south-west* GPS2 also accelerate, albeit with a lower magnitude. The northern GPS (GPS1 and GPS4) show anomalous motion in the north-south plane

Rapid lake tapping, W. Greenland

S. H. Doyle et al.

Title Page

Abstract

Introduction

Conclusions

References

Tables

Figures

◀

▶

◀

▶

Back

Close

Full Screen / Esc

Printer-friendly Version

Interactive Discussion



including transient reverse ice flow at GPS1. The mean daily vector for the 29 June is of a lower magnitude for the western GPS compared to the eastern GPS, implying a compressive strain regime that is also evident in the decreasing separations between GPS 1–3, 1–4 and 2–3 (Fig. 6a, b and f).

A detailed time series of discharge (Q), rate of discharge (dQ/dt), uplift (Z) and rate of uplift (dZ/dt) is presented in Fig. 7. On 30 June 2010 at 01:15 the uplift rate at GPS2 suddenly increases leading to a maximum 0.34 m of uplift at 02:09. In this period, GPS 1 and 4 are uplifted by 0.07 m and 0.1 m, respectively and there is no discernible uplift at GPS3. Coincident with the start of rapid discharge at 01:40 the uplift rate at *north-west* GPS1 increases. In the interval 01:40–02:00, the lake volume decreases by $1.75 \times 10^5 \text{ m}^3$ (2.4%) and GPS1 and GPS2 move north-west (Fig. 5a and b) with slight compression (Fig. 6c). At 02:00 *north-west* GPS1 continues to move in the north-west direction, accelerating and reaching a maximum displacement to the north of 0.3 m. At 02:00, GPS2 reverses in direction moving to the south-west coincident with a step increase in the discharge, seismicity, uplift rate at GPS1, and separation rate between all the GPS with the exception of GPS 2–3 (Figs. 5, 6, 7 and 8). Rapid GPS separation continues until 03:00 when *south-west* GPS2 reverses to the north and *north-west* GPS1 reverses to the south, causing the separation rates to become negative (Fig. 8c). The maximum discharge Q_{max} of $3300 \text{ m}^3 \text{ s}^{-1}$ occurs at 02:47 simultaneous with the peak uplift rate at GPS1 of 0.8 m h^{-1} . Figure 6 shows that the maximum relative separation between GPS 1–2, 1–3, 1–4 and 2–4 is attained at 03:00, simultaneous with a lull in seismicity across all six seismometers (Fig. 8) and a transient $1 \text{ m}^3 \text{ s}^{-2}$ increase in the discharge rate (dZ/dt) which remains negative (Fig. 7b). At 03:00 there is a short-lived (15-min) period of uplift at GPS2. Post 03:00, inter-GPS separations decrease as the discharge reduces. Rapid discharge ends at 03:15 with $V = 4.8 \times 10^4 \text{ m}^3$ (0.65% remaining). Peak uplift at GPS1 of 0.9 m isn't reached until 03:40. Following peak uplift, GPS1 subsides at a gradually reducing rate (mean uplift rate of -0.07 m h^{-1}) remaining 0.3 m above its pre-tapping elevation by the end of 30 June 2010. Accordingly, GPS2, GPS3 and GPS4 remain uplifted by 0.1 m, 0.18 m and 0.24 m, respectively.

**Rapid lake tapping,
W. Greenland**

S. H. Doyle et al.

Title Page

Abstract

Introduction

Conclusions

References

Tables

Figures

◀

▶

◀

▶

Back

Close

Full Screen / Esc

Printer-friendly Version

Interactive Discussion



5 4 Discussion

On the basis of the observations described above, the rapid in situ tapping of Lake F on the 30 June 2010 can be decomposed into three episodes: initial drainage (01:40–02:00); fracture opening (02:00–03:00); and fracture closure (03:00–03:15). These episodes are bounded by the duration of rapid discharge and it is likely some opening and closure of fractures occurred outside of these episodes. The horizontal and vertical GPS velocities during each episode are illustrated on Fig. 9. The timings of each episode together with the time of Q_{\max} are indicated on Figs. 5, 6 and 7.

Episode 1, initial drainage, begins at the onset of rapid drainage and ends when GPS2 changes direction to the south causing north-south extension across the lake (Fig. 9a). In episode 1, a small (2.4 %) amount of water drains resulting in surface uplift concentrated at GPS2. In episode 1, there is an increase in seismicity for the western half of the seismic array (S1–3) but little or no increase for the eastern seismometers (S4–6, see Fig. 8).

As the fractures open in episode 2 the discharge rapidly increases. The divergence of GPS 1–3, 1–2, 3–4 and 2–4 (Fig. 6a, c, d and e) are interpreted as the opening of the main fracture F1 (Fig. 9b). Likewise, short-term longitudinal extension between GPS1 and GPS4 of ~ 0.2 m (see Fig. 6b), involving the reverse motion of GPS4 commencing at 02:00, is interpreted as the opening of subsidiary fracture F2. The circular path of GPS4 during lake tapping (see Fig. 5d) is the combined effect of fractures F1 and F2 opening and closing. The transient reverse motion of GPS4 demonstrates the difficulty in opening up a transverse fracture – as soon as rapid discharge ends, GPS4 moves back to the west and the fracture closes. The maximum rate of surface uplift (dZ/dt) for GPS1 occurred at 02:47 simultaneous with the peak discharge, providing conclusive evidence that surface water rapidly attained the ice-bed interface.

At 03:00, the boundary between episode 2 and 3, the fractures attain their maximum width and the short respite in fracturing is responsible for a lull in seismicity evident in the records for all six seismometers (Fig. 8). This quiescence suggests that seismicity is

TCD

6, 3863–3889, 2012

Rapid lake tapping, W. Greenland

S. H. Doyle et al.

Title Page

Abstract

Introduction

Conclusions

References

Tables

Figures

◀

▶

◀

▶

Back

Close

Full Screen / Esc

Printer-friendly Version

Interactive Discussion



predominantly generated by the deformation of ice during fracture opening and closing and not by water flow which is continuing at a high rate ($Q = 1450 \text{ m}^3 \text{ s}^{-1}$). Immediately after 03:00 a step-increase in seismicity, particularly evident at seismometer S4 (Fig. 8j), is seen as the fracture begins to close. Post 03:15 the inter-GPS separation rate between GPS 1–3, 1–4, 1–2, 3–4 and 2–4 become negative as the fractures close (Fig. 6 and 9c).

In episode 3, fractures begin to close as the discharge and uplift reduces. The highest magnitude seismicity (greatest normalised RMS amplitude) occurs in episode 3 when the fractures are closing and not in episode 2 when the fractures are opening. By the end of rapid drainage at 03:15 the fractures are effectively closed (Fig. 6).

After attaining peak uplift of 0.9 m at 03:30 GPS1 gradually subsides by 0.1 m over 5 h. Peak uplift occurs earlier but with a lower magnitude for GPS2, GPS3 and GPS4. Throughout the lake tapping event the vertical motion of GPS2, in contrast to the motion of GPS1, GPS3 and GPS4, is characterised by sudden steps, two of which are coincident with the start and end of the fracture opening episode. This could indicate that the vertical motion of GPS2 is driven by discrete fracturing events rather than by hydraulic jacking alone.

The characteristics of the rapid tapping of Lake F are consistent with Das et al. (2008) who observed the rapid (1.4 h) drainage of a $4.4 \times 10^7 \text{ m}^3$ supraglacial lake through 980 m of the western margin of the Greenland Ice Sheet at 68.7° N . The reverse and circular motion of the singular GPS of Das et al. is comparable to that of GPS4, which was similarly located on westerly flowing ice, north of a longitudinal fracture and west of a transverse fracture. The reverse and circular motion of the singular GPS of Das et al. are comparable to those of GPS4 which was similarly located on westerly flowing ice, north of a longitudinal fracture and west of a transverse fracture. The step-increases in seismicity observed during the tapping of Lake F (see Fig. 8) are also comparable (see Fig. S3 of Das et al., 2008).

Based on the locations of F1 and F2, we conceptualise the ice-mass structurally into three semi-independent blocks: the southern, north-eastern and north-western. The

**Rapid lake tapping,
W. Greenland**

S. H. Doyle et al.

Title Page

Abstract

Introduction

Conclusions

References

Tables

Figures

◀

▶

◀

▶

Back

Close

Full Screen / Esc

Printer-friendly Version

Interactive Discussion



**Rapid lake tapping,
W. Greenland**

S. H. Doyle et al.

Title Page

Abstract

Introduction

Conclusions

References

Tables

Figures

◀

▶

◀

▶

Back

Close

Full Screen / Esc

Printer-friendly Version

Interactive Discussion



gradients of hydraulic potential were calculated from basal and surface elevation data collected by skidoo-based radio echo sounding (Lindback and Pettersson, unpublished data) assuming basal water pressures were everywhere equal to the ice overburden pressure (Shreve, 1972). Figure 10 indicates that subglacial water delivered to the ice-bed interface below moulin M1 would be preferentially routed to the north-west. The higher magnitude peak uplift of 0.9 m at *north-west* GPS1 compared to 0.09 m at *south-east* GPS3 supports this assertion. The direction of dip of sub-vertical fractures F1 and F2 to the north and west, respectively (see Fig. 2) and the permanent offset of the northern wall above the southern wall of F1, suggest the northern-western block was preferentially uplifted. Figure 10 suggests that the motion of the north-eastern and southern blocks would be restricted by their location on basal topographic highs. Additionally, Fig. 8 demonstrates that during lake tapping the greatest normalised RMS amplitude was recorded by the most western seismometers (S1–3) corroborating with the GPS observation of the greatest horizontal and vertical motion of the north-western block on which GPS1 was located (Fig. 5a and e).

4.1 Fracture analysis

Assuming first, that the inter-GPS separation is entirely a result of fracturing and second that the fractures are U-shaped with constant width, we can estimate the cross-sectional area, volume and water velocity through the fractures at the time of peak separation (03:00). Interpolating the maximum separations between GPS 1–2, 1–3, 2–4 and 3–4 over fracture, F1's, 2.6 km wetted length gives a mean fracture width at peak separation of 0.4 m and an estimated maximum cross-sectional area of 842 m². This fracture width agrees well with the modelling results of Krawczynski et al. (2009) that suggest an idealised conical lake of a similar size to Lake F (diameter = 2.2 km, area = 3.8 km²) would drain via a 0.4 m wide fracture across the width of the lake in ~2 h.

With a length of 700 m and a peak separation of 0.2 m the maximum cross-sectional area of F2 is estimated at 140 m². Combined, F1 and F2 have a total cross-sectional

5 area at 03:00 of 982 m^2 . Dividing the discharge at 03:00 ($Q = 1450 \text{ m}^3 \text{ s}^{-1}$) by the
combined cross-sectional area gives a flow velocity of 1.5 ms^{-1} . Hence, due to the
length of the fractures, rapid discharge can be achieved by combining reasonable wa-
ter velocities with sub-metre fracture widths. The total volume of the fractures at 03:00,
assuming an ice thickness of 1100 m, is $1.1 \times 10^6 \text{ m}^3$ or 15 % of the lakes volume prior
to tapping. The actual volume of water that drained between 01:40 and 03:00 is much
10 larger at $6.8 \times 10^6 \text{ m}^3$.

4.2 Initiation mechanism

Alley et al. (2005) assert that the tensile stress caused by the acceleration of down-
stream ice is important for initiating a hydrofracture. Prior to the tapping of Lake F there
is no evidence for longitudinal extension across the main fracture. On 29 June, differ-
ential acceleration of the eastern GPS (3 and 4) compared to the western GPS (1 and
15 2) causes the longitudinal strain regime to be compressive (Fig. 6b and f). Immediately
preceding tapping, there is also differential motion of the northern GPS (1 and 4) in
relation to the southern (2 and 3, Fig. 6c and d) suggesting that pure shear (shear with
compression) could be occurring along F1 prior to the transverse north-south exten-
sion during hydraulic fracture. These observations agree with Krawczynski et al. (2009)
20 who found that water-filled crevasses can propagate without longitudinal tension and
that a given volume of water has the propensity to propagate a water-filled crack further
in regions with less tension (or even slight compression), as thinner cracks require less
water to remain water filled.

25 5 Conclusions

To investigate the immediate characteristics of rapid in situ lake tapping events through
kilometre thick ice on the Greenland Ice Sheet we compare the differential motion
of four GPS located around an annually tapping supraglacial lake with records of

Rapid lake tapping, W. Greenland

S. H. Doyle et al.

Title Page

Abstract

Introduction

Conclusions

References

Tables

Figures

◀

▶

◀

▶

Back

Close

Full Screen / Esc

Printer-friendly Version

Interactive Discussion



**Rapid lake tapping,
W. Greenland**

S. H. Doyle et al.

Title Page

Abstract

Introduction

Conclusions

References

Tables

Figures

◀

▶

◀

▶

Back

Close

Full Screen / Esc

Printer-friendly Version

Interactive Discussion



discharge and passive seismicity. Ice motion during rapid tapping is dominated by the opening and closure of a 3 km long fracture, suggesting that on short time-scales the brittle fracture of ice can dominate ice motion and play an important role in ice sheet hydrology.

The maximum recorded uplift rate of 0.8 m h^{-1} occurred at GPS1 simultaneous to the maximum discharge ($3300 \text{ m}^3 \text{ s}^{-1}$), providing evidence that water rapidly attained the ice-bed interface. The greatest horizontal displacement and vertical uplift was observed above the preferential subglacial drainage route below GPS1 suggesting that basal topography and the gradient of hydraulic potential exert control on water routing, ice motion, uplift and fracturing.

The kilometre-scale length of the fractures allows rapid discharge to be achieved by combining reasonable water velocities with sub-metre fracture widths. Our observations of pre-tapping longitudinal compression agree with Krawczynski et al. (2009) who assert that water-filled crevasses can propagate in areas without longitudinal extension.

The drainage of Lake F occurred ~ 3 to 4 weeks earlier in abnormally warm years suggesting that in a warming climate, surface water will reach the ice-bed interface earlier. The rapid drainage of a cluster of several lakes in the same elevation band, including Lake F, was coincident with an isolated peak in the discharge of catchment-wide proglacial Watson River.

Acknowledgements. The research was funded by the Greenland Analogue Project, Sub-Project A and by UK Natural Environment Research Council (NERC) research grants NE/G007195/1 and NE/G005796/1. The seismic instruments were provided by Seis-UK at the University of Leicester. S.H.D. is supported by an Aberystwyth University doctoral scholarship. C.F.D. and A.F. are supported by NERC doctoral scholarships and G.A.J. is supported by NERC research grant NE/G007195/1. Ian Batholomew and Matt King are thanked for advice on GPS processing. Christian Helanow, Adam Booth and Henry Patton are thanked for assistance in the field. Nolwenn Chauché is thanked for helpful discussion. TEQC software was used to convert the raw GPS data to Receiver INdependent EXchange (RINEX) format (Estey and Meertens, 1999). MODIS data are distributed by the Land Processes Distributed Active Archive Center

(LP DAAC), located at the USGS EROS Center (<http://lpdaac.usgs.gov>). Landsat data are distributed by the US Geological Survey (<http://glovis.usgs.gov>).

References

- 10 Alley, R., Dupont, T., Parizek, B., and Anandakrishnan, S.: Access of surface meltwater to beds of sub-freezing glaciers: preliminary insights, *Ann. Glaciol.*, 40, 8–13, 2005.
- Bamber, J., Alley, R., and Joughin, I.: Rapid response of modern day ice sheets to external forcing, *Earth Planet. Sc. Lett.*, 27, 1–13, 2007.
- Bartholomew, T., Anderson, R., and Anderson, S.: Response of glacier motion to transient water storage, *Nat. Geosci.*, 1, 33–37, 2008.
- 15 Bartholomew, I., Nienow, P., Sole, A., Mair, D., Cowton, T., King, M., and Palmer, S.: Seasonal variations in Greenland Ice Sheet motion: inland extent and behaviour at higher elevations, *Earth Planet. Sc. Lett.*, 307, 271–278, 2011.
- Boon, S. and Sharp, M.: The role of hydrologically-driven ice fracture in drainage system evolution on an Arctic glacier, *Geophys. Res. Lett.*, 30, 1–4, doi:10.1029/2003GL018034, 2003.
- 20 Box, J. and Ski, K.: Remote sounding of Greenland supraglacial melt lakes: implications for subglacial hydraulics, *J. Glaciol.*, 53, 257–265, 2007.
- Cappelen, J.: DMI Monthly Climate Data Collection 1768–2010, Denmark, The Faroe Islands and Greenland, Tech. Rep. 11–05, Danish Meteorological Institute, 2011.
- Cappelen, J., Jørgensen, B., Laursen, E., Stannius, L., and Thomsen, R.: The observed climate of Greenland, 1958–99 – with climatological standard normals, 1961–90., Tech. Rep. 00–18, Danish Meteorological Institute, 2001.
- 25 Chen, G.: GPS kinematic positioning for the airborne laser altimetry at Long Valley, California, Ph. D. thesis, Mass. Inst. of Technol., Cambridge, available at: <http://dspace.mit.edu/bitstream/handle/1721.1/9680/42583460.pdf?sequence=1>, 1998.
- 30 Das, S., Joughin, I., Behn, M., Howat, I., King, M., Lizarralde, D., and Bhatia, M.: Fracture propagation to the base of the Greenland Ice Sheet during supraglacial lake drainage, *Science*, 320, 778–781, 2008.
- Dow, J., Neilan, R. E., and Rizos, C.: The International GNSS Service in a changing landscape of Global Navigation Satellite Systems, *J. Geodesy*, 83, 191–198, doi:10.1007/s00190-008-0300-3, 2009.

Rapid lake tapping, W. Greenland

S. H. Doyle et al.

Title Page

Abstract

Introduction

Conclusions

References

Tables

Figures

◀

▶

◀

▶

Back

Close

Full Screen / Esc

Printer-friendly Version

Interactive Discussion



**Rapid lake tapping,
W. Greenland**

S. H. Doyle et al.

Title Page

Abstract

Introduction

Conclusions

References

Tables

Figures

◀

▶

◀

▶

Back

Close

Full Screen / Esc

Printer-friendly Version

Interactive Discussion



- 5 Echelmeyer, K., Clarke, T., and Harrison, W.: Surficial glaciology of Jakobshavn Isbrae, West Greenland: Part I. Surface morphology, *J. Glaciol.*, 37, 368–382, 1991.
- Estey, L. and Meertens, C.: TEQC: The multi-purpose toolkit for GPS/GLONASS data, *GPS Solut.*, 3, 42–29, 1999.
- Georgiou, S., Shepherd, A., McMillan, M., and Nienow, P.: Seasonal evolution of supraglacial lake volume from ASTER imagery, *Ann. Glaciol.*, 50, 95–100, 2009.
- 10 Herring, T., King, R., and McClusky, S.: GAMIT Reference Manual, Release 10.4, Massachusetts Institute of Technology, Cambridge, available at: http://www-gpsg.mit.edu/~simon/gtgk/GAMIT_Ref.pdf, 2010.
- Hoffman, M., Catania, G., Neumann, T., Andrews, L., and Rumrill, J.: Links between acceleration, melting, and supraglacial lake drainage of the Western Greenland Ice Sheet, *J. Geophys. Res.*, 116, F04035, doi:10.1029/2010JF001934, 2011.
- 15 Krawczynski, M., Behn, M., Das, S., and Joughin, I.: Constraints on the lake volume required for hydro-fracture through ice sheets, *Geophys. Res. Lett.*, 36, 1–5, 2009.
- McMillan, M., Nienow, P., Shepherd, A., Benham, T., and Sole, A.: Seasonal evolution of supraglacial lakes on the Greenland Ice Sheet, *Earth Planet. Sc. Lett.*, 262, 484–492, 2007.
- 20 Palmer, S., Shepherd, A., Nienow, P., and Joughin, I.: Seasonal speedup of the Greenland Ice Sheet linked to routing of surface water, *Earth Planet. Sc. Lett.*, 302, 423–428, doi:10.1016/j.epsl.2010.12.037, 2011.
- Pimental, S. and Flowers, G.: A numerical study of hydrologically driven glacier dynamics and subglacial flooding, *P. Roy. Soc.*, 467, 537–558, doi:10.1098/rspa.2010.0211, 2010.
- 25 Pritchard, H., Arthern, R., Vaughan, D., and Edwards, L.: Extensive dynamic thinning on the margins of the Greenland and Antarctic ice sheets, *Nature*, 461, 971–975, doi:10.1038/nature08471, 2009.
- Selmes, N., Murray, T., and James, T.: Fast draining lakes on the Greenland Ice Sheet, *Geophys. Res. Lett.*, 38, L15501, doi:10.1029/2011GL047872, 2011.
- 30 Shepherd, A., Hubbard, A., Nienow, P., King, M., McMillan, M., and Joughin, I.: Greenland ice sheet motion coupled with daily melting in late summer, *Geophys. Res. Lett.*, 36, 1–4, doi:10.1029/2008GL035758, 2009.
- Shreve, R.: Movement of water in glaciers, *J. Glaciol.*, 11, 205–214, 1972.
- van As, D., Hubbard, A. L., Hasholt, B., Mikkelsen, A. B., van den Broeke, M. R., and Fausto, R. S.: Large surface meltwater discharge from the Kangerlussuaq sector of the

**Rapid lake tapping,
W. Greenland**

S. H. Doyle et al.

Title Page

Abstract

Introduction

Conclusions

References

Tables

Figures

I◀

▶I

◀

▶

Back

Close

Full Screen / Esc

Printer-friendly Version

Interactive Discussion



Greenland ice sheet during the record-warm year 2010 explained by detailed energy balance observations, *The Cryosphere*, 6, 199–209, doi:10.5194/tc-6-199-2012, 2012.

van de Wal, R., Boot, W., van den Broeke, M., Smeets, C., Reijmer, C., Donker, J., and Oerlemans, J.: Large and rapid melt-induced velocity changes in the ablation zone of the Greenland Ice Sheet, *Science*, 321, 111–113, 2008.

van der Veen, C.: Fracture propagation as means of rapidly transferring meltwater to the base of glaciers, *Geophys. Res. Lett.*, 34, L01501, doi:10.1029/2006GL028385, 2007.

Weertman, J.: Can a water filled crevasse reach the bottom surface of a glacier? *Union Geodésique et Géophysique Internationale. Association Internationale d'Hydrologie Scientifique. Commission de Neiges et Glaces. Symposium on the Hydrology of Glaciers, Cambridge, 7–13 September 1969, Publication No. 95 de l'Association Internationale d'Hydrologie Scientifique*, 139-45, 1973.

Zwally, J., Abdalati, W., Herring, T., Larson, K., Saba, J., and Steffen, K.: Surface melt-induced acceleration of Greenland Ice-Sheet Flow, *Science*, 297, 218–222, 2002.

Rapid lake tapping,
W. Greenland

S. H. Doyle et al.

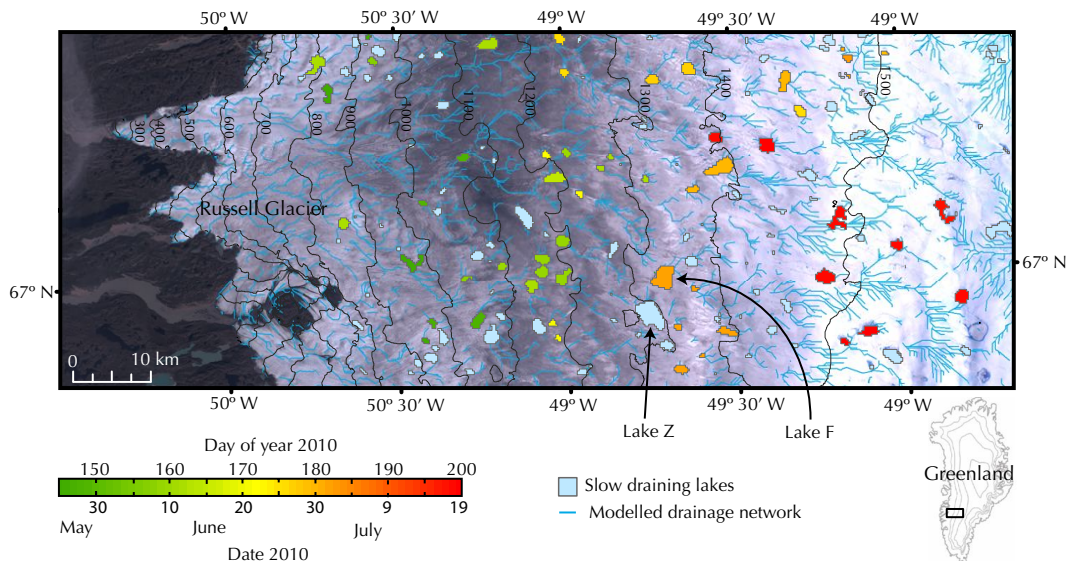


Fig. 1. The maximum extent of supraglacial lakes within the Russell Glacier catchment during the 2010 melt-season and the location of the Field Site, Lake F. The green-red colour scheme indicates the timing of rapidly draining (< 4 days) lakes, with slow-draining (> 4 days) lakes in blue. The modelled supraglacial drainage network is shown. The background is a 15 m resolution Landsat image acquired on the 18 August 2010.

Title Page

Abstract

Introduction

Conclusions

References

Tables

Figures

◀

▶

◀

▶

Back

Close

Full Screen / Esc

Printer-friendly Version

Interactive Discussion



Rapid lake tapping,
W. Greenland

S. H. Doyle et al.

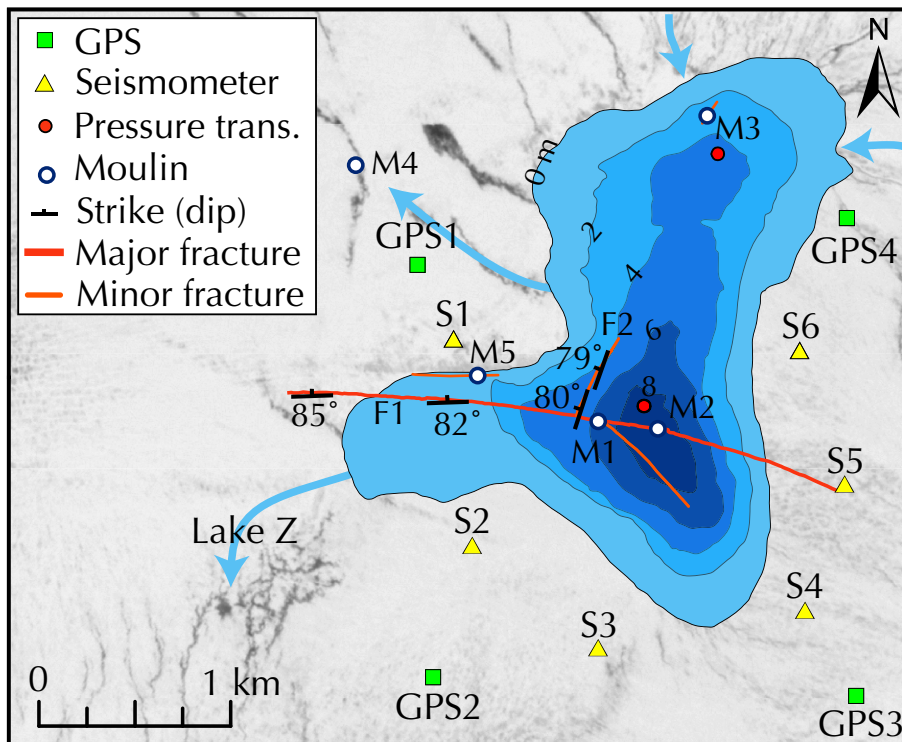


Fig. 2. Map of Lake F showing: the instrument array; the fractures and moulins surveyed post-drainage; and the lake perimeter and depth immediately before rapid tapping. The background image is a 5 m resolution SPOT image acquired 7 July 2008. The main supraglacial rivers entering and leaving Lake F are shown by blue arrows.

Title Page

Abstract

Introduction

Conclusions

References

Tables

Figures

◀

▶

◀

▶

Back

Close

Full Screen / Esc

Printer-friendly Version

Interactive Discussion



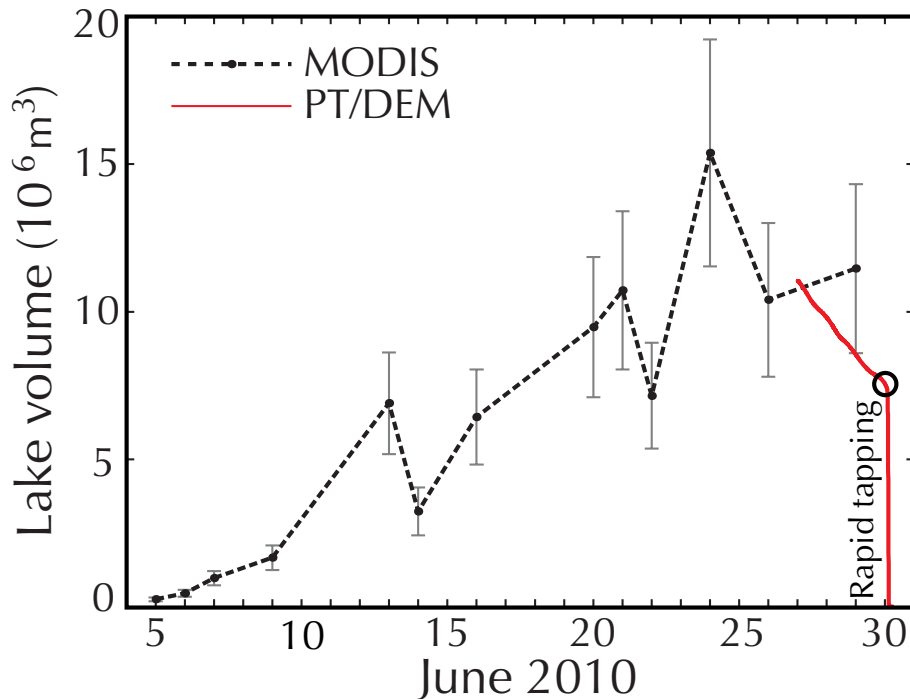


Fig. 3. Time series of Lake F volume in 2010 estimated from MODIS and the pressure transducer (PT)/digital elevation model (DEM) calculations. The transition from slow drainage to rapid tapping is indicated by the black circle. Error bars indicate the uncertainty range of the lake volumes calculated from MODIS.

**Rapid lake tapping,
W. Greenland**

S. H. Doyle et al.

Title Page	
Abstract	Introduction
Conclusions	References
Tables	Figures
◀	▶
◀	▶
Back	Close
Full Screen / Esc	
Printer-friendly Version	
Interactive Discussion	



**Rapid lake tapping,
W. Greenland**

S. H. Doyle et al.

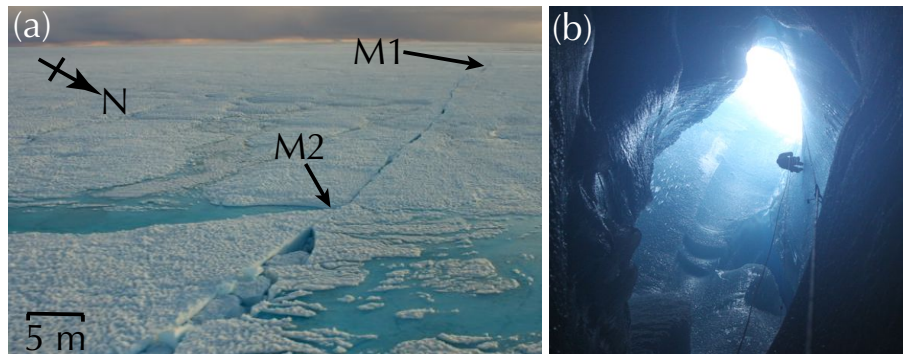


Fig. 4. Photos of Lake F post-drainage: **(a)** the main fracture 8 days after lake tapping showing the location of moulins M1 and M2 with the deepest region of the lake located 10 m east of M2; and **(b)** the largest moulin M1, ~ 10 m in diameter. Fallen ice blocks blocked the moulin at 45 m below the surface.

[Title Page](#)[Abstract](#)[Introduction](#)[Conclusions](#)[References](#)[Tables](#)[Figures](#)[I◀](#)[▶I](#)[◀](#)[▶](#)[Back](#)[Close](#)[Full Screen / Esc](#)[Printer-friendly Version](#)[Interactive Discussion](#)

Rapid lake tapping,
W. Greenland

S. H. Doyle et al.

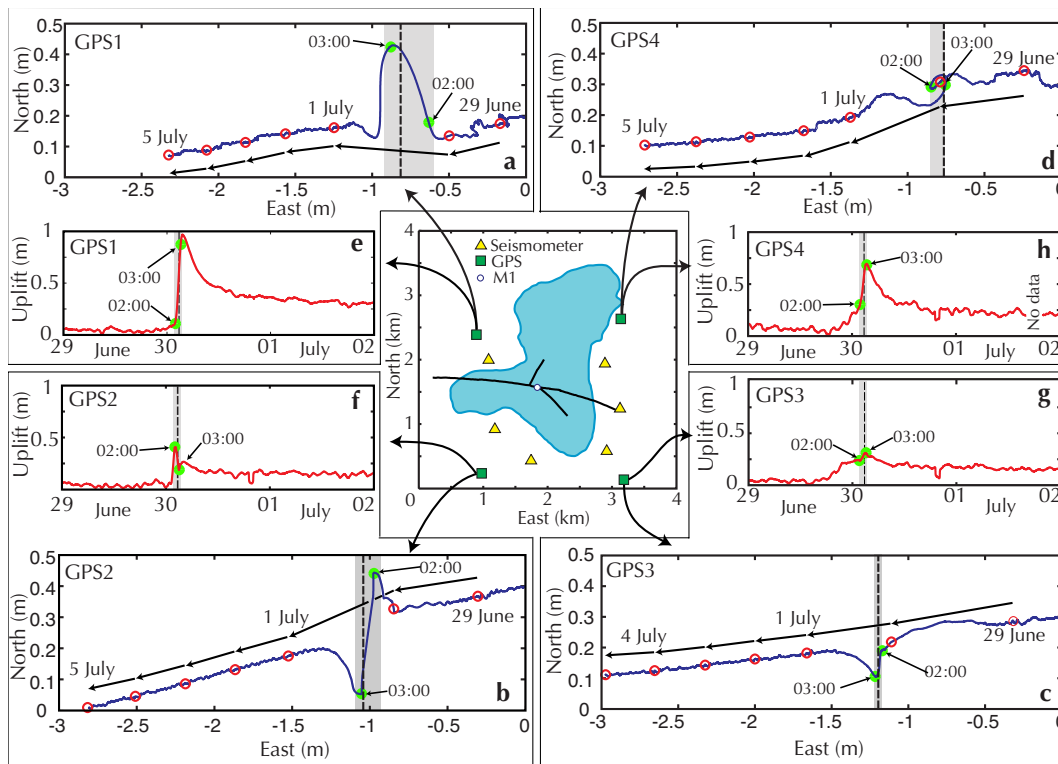


Fig. 5. Horizontal and vertical motion of the four GPS. Plots (a–d) are plan views of the horizontal GPS motion and (e–h) are time series of vertical GPS uplift. To emphasise the transverse motion the y-axes of (a–d) are exaggerated by a factor of 2. On (a–d) hollow red circles indicate day boundaries and arrows represent daily vectors. On (a–h) solid green circles indicate the times of 02:00 and 03:00; the grey shade indicates the period of rapid ($Q > 50 \text{ m}^3 \text{ s}^{-1}$) discharge; and the vertical dashed line indicates the time of maximum discharge Q_{max} .

Title Page

Abstract

Introduction

Conclusions

References

Tables

Figures

◀

▶

◀

▶

Back

Close

Full Screen / Esc

Printer-friendly Version

Interactive Discussion



Rapid lake tapping,
W. Greenland

S. H. Doyle et al.

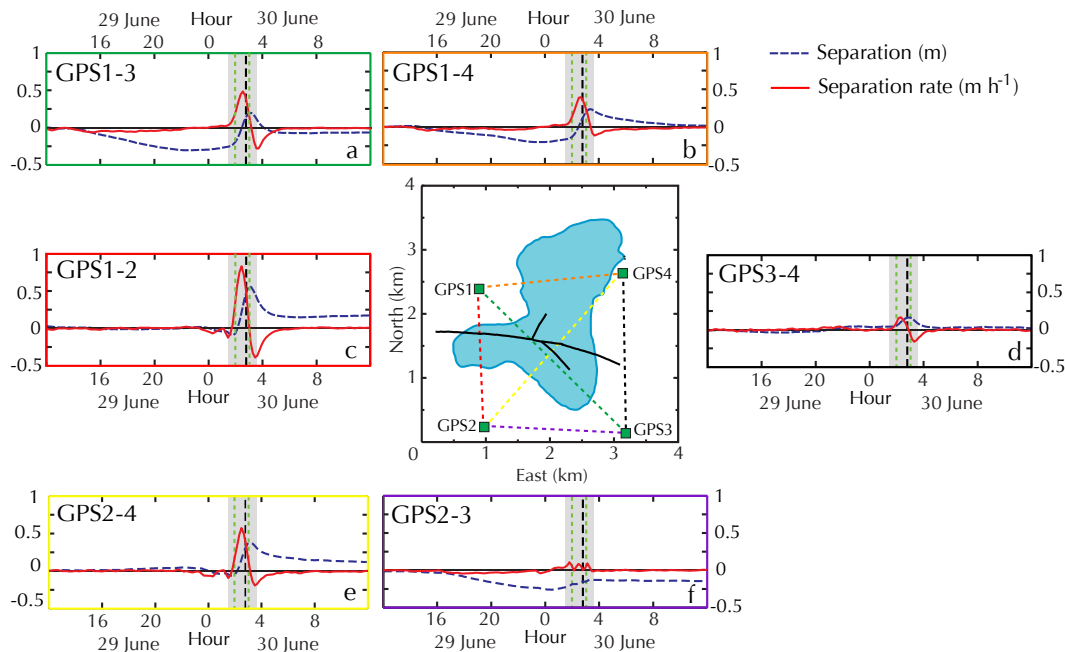


Fig. 6. Inter-GPS separation (blue dashed line) and rate of separation (solid red line). The colour of the axes correspond to the dashed lines on the central map. The grey shade indicates the time of rapid ($Q > 50 \text{ m}^3 \text{ s}^{-1}$) discharge, the black dashed line indicates the time of peak discharge Q_{max} and the green dashed lines indicate the times of 02:00 and 03:00.

Title Page

Abstract

Introduction

Conclusions

References

Tables

Figures

◀

▶

◀

▶

Back

Close

Full Screen / Esc

Printer-friendly Version

Interactive Discussion



Rapid lake tapping,
W. Greenland

S. H. Doyle et al.

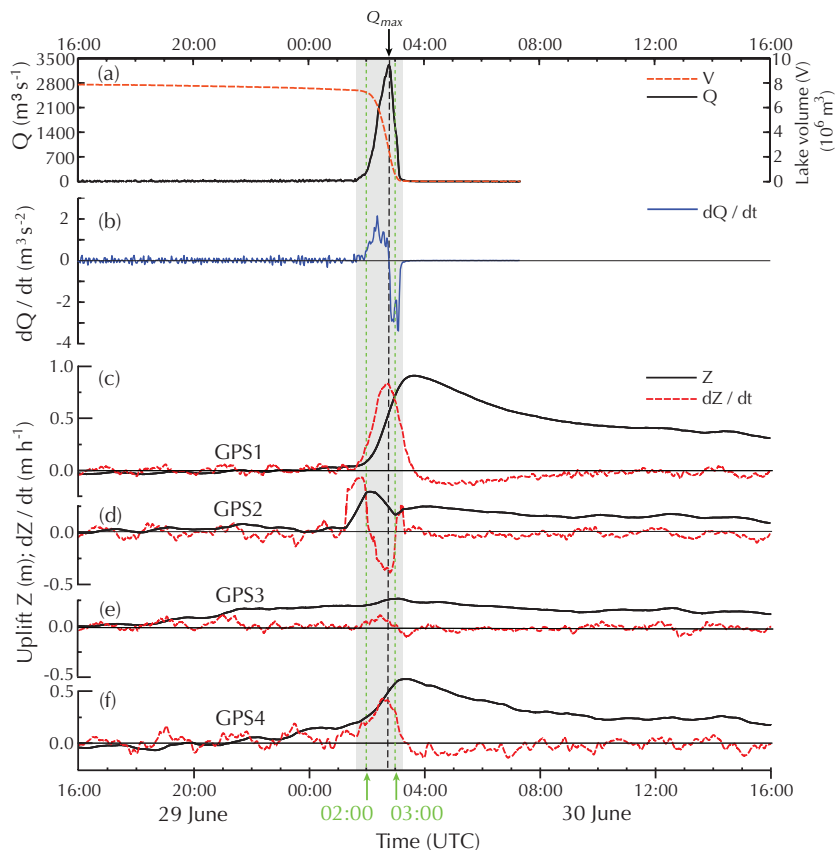


Fig. 7. Time series of **(a)** volume V and discharge Q **(b)** rate of discharge dQ/dt and **(c–f)** uplift Z and the rate of uplift dZ/dt for GPS 1 to 4. The grey shade indicates the time of rapid ($Q > 50 \text{ m}^3 \text{ s}^{-1}$) discharge. The black dashed line indicates the time of peak discharge Q_{\max} and the green dashed lines indicates the times of 02:00 and 03:00.

Title Page

Abstract

Introduction

Conclusions

References

Tables

Figures

◀

▶

◀

▶

Back

Close

Full Screen / Esc

Printer-friendly Version

Interactive Discussion



Rapid lake tapping,
W. Greenland

S. H. Doyle et al.

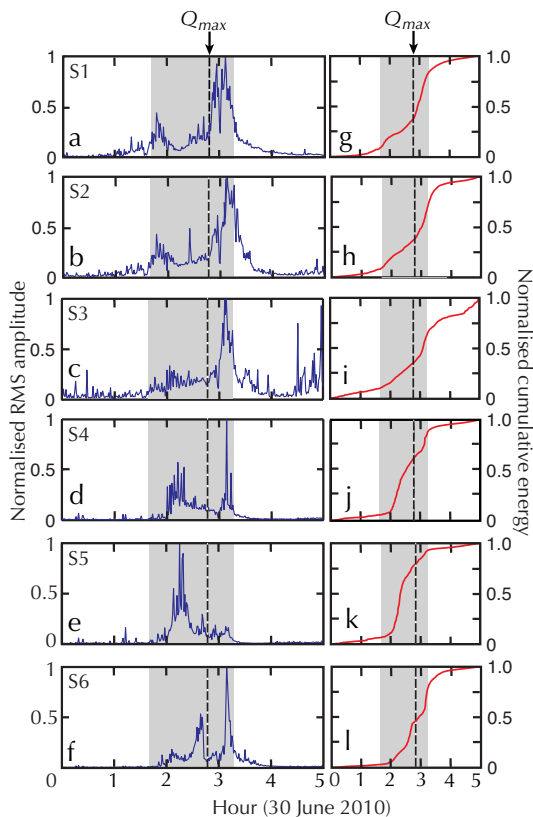


Fig. 8. Normalised seismic RMS amplitude (a–f) and normalised seismic cumulative energy (g–l) for the passive seismic array ordered anti-clockwise from west (S1) to east (S6). The time of rapid ($Q > 50 \text{ m}^3 \text{ s}^{-1}$) discharge (grey shade) and the time of maximum discharge (dashed vertical line) are indicated.

Title Page

Abstract Introduction

Conclusions References

Tables Figures

◀ ▶

◀ ▶

Back Close

Full Screen / Esc

Printer-friendly Version

Interactive Discussion



Rapid lake tapping,
W. Greenland

S. H. Doyle et al.

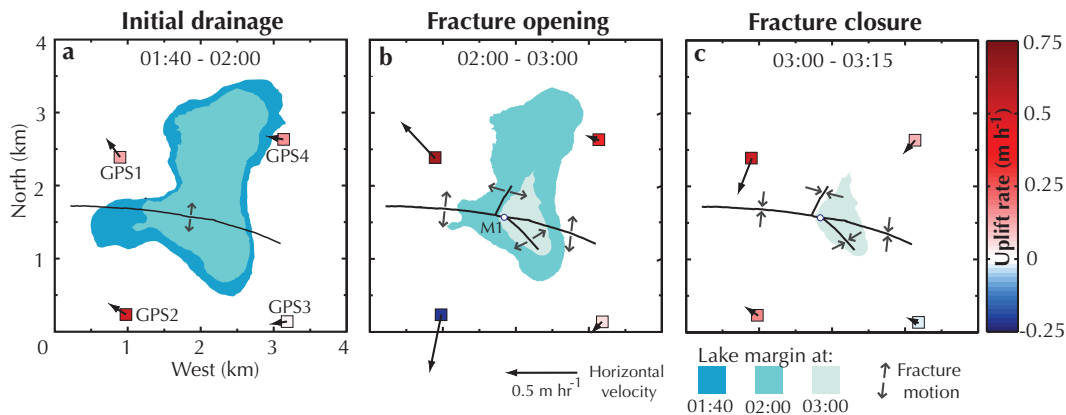


Fig. 9. Horizontal and vertical GPS velocities during the three episodes of Lake F's rapid drainage: **(a)** initial drainage; **(b)** fracture opening; and **(c)** fracture closure. Arrows represent horizontal velocity vectors. The colour of each GPS symbol represents the mean uplift rate. The lake margin at each time step is shown.

Title Page

Abstract

Introduction

Conclusions

References

Tables

Figures

◀

▶

◀

▶

Back

Close

Full Screen / Esc

Printer-friendly Version

Interactive Discussion



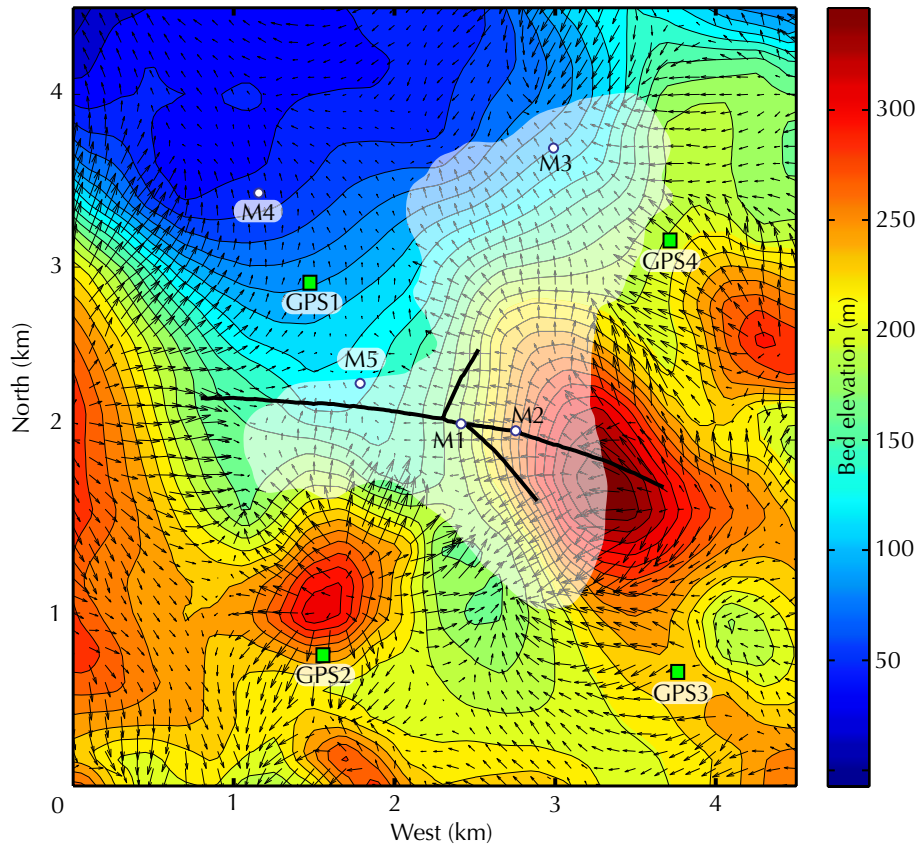


Fig. 10. Map of the hydraulic potential gradients and subglacial topography for Lake F. The arrows show the direction and relative magnitude of the hydraulic potential gradients. The lake margin immediately prior to lake tapping is shown together with the locations of moulins, fractures and GPS. The contour interval is 10 m.

**Rapid lake tapping,
W. Greenland**

S. H. Doyle et al.

Title Page

Abstract Introduction

Conclusions References

Tables Figures

◀ ▶

◀ ▶

Back Close

Full Screen / Esc

Printer-friendly Version

Interactive Discussion

